

PROBING THE VALENCE QUARK REGION OF
NUCLEONS WITH Z BOSONS AT LHCb*

TIANQI LI

on behalf of the LHCb Collaboration

Guangdong Provincial Key Laboratory of Nuclear Science
Guangdong-Hong Kong Joint Laboratory of Quantum Matter
Institute of Quantum Matter, South China Normal University, Guangzhou, China

*Received 29 July 2022, accepted 20 August 2022,
published online 14 December 2022*

Due to its forward coverage, the LHCb can probe the valence quark distributions of protons and nuclei at small and large Bjorken- x with high precision. These proceedings present new LHCb measurements of Z -boson production in association with charm jet in the forward region of proton–proton collisions and Z -boson production in proton–lead collisions. Z +charm-jet production could be sensitive to a valence-like intrinsic-charm component in the proton wave function. The measurements of Z production in proton–lead collisions provide new constraints on the partonic structure of nucleons inside nuclei. Comparisons between the results and calculations with parton distribution functions are also discussed.

DOI:10.5506/APhysPolBSupp.16.1-A126

1. Introduction

The LHCb detector [1, 2], optimized for studying heavy-flavour physics in proton–proton (pp) collisions at the LHC, is a single-arm forward spectrometer covering the pseudorapidity range $2 < \eta < 5$, providing a high momentum resolution down to very low transverse momentum (p_T), excellent reconstruction, and particle identification. Due to the forward acceptance, the LHCb results are highly complementary to the other LHC experiments. The LHCb participated successfully in the recording of proton–lead data samples in 2013, thus becoming a member of the LHC heavy-ion program to provide unique datasets for heavy-ion physics studies. As shown in Fig. 1, the LHCb provides data that can constrain nuclear parton distribution functions (nPDFs) in both low- x and high- x regions. The measurements

* Presented at the 29th International Conference on Ultrarelativistic Nucleus–Nucleus Collisions: Quark Matter 2022, Kraków, Poland, 4–10 April, 2022.

of Z -boson production at LHCb can provide constraints at high momentum transfer (Q^2). Furthermore, the LHCb measurements of Z +charm-jet production provide information on the quark PDFs at large- x region relevant to studies of intrinsic charm.

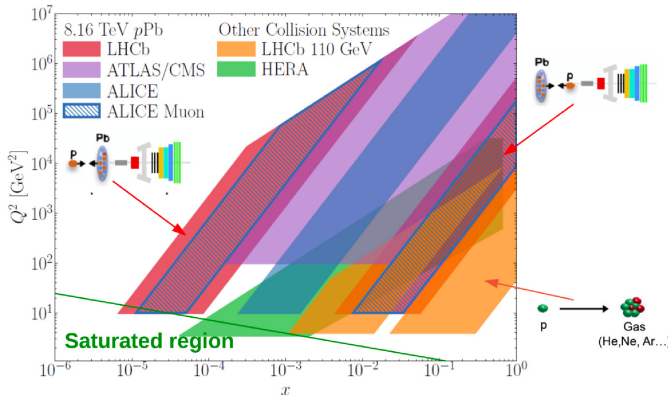


Fig. 1. Kinematic regions corresponding to the acceptance of the four LHC experiments in p -Pb collisions.

In this article, we report on recent results of the Z bosons produced in association with charm in the forward region [3] and the Z -boson production in the proton-lead collisions [4] measured by the LHCb Collaboration.

2. Probe intrinsic charm: Zc production in proton-proton collisions

The possibility that the proton wave function may contain an intrinsic-charm (IC) component, in addition to the c -quark content due to perturbative gluon radiation, has been an interesting topic in recent years (see Ref. [5] for a review). Light front QCD calculations (Refs. [6, 7]) predict the presence of the non-perturbative IC can manifest in valence-like charm content in the parton distribution function, whereas, if the charm is entirely perturbative, the charm PDF should rapidly decrease at large Bjorken- x . The goal is to use a high-precision measurement of an observable with direct sensitivity to large- x charm to probe IC in proton, where Q is large enough for the hadronic and nuclear effects to be negligible.

Reference [8] proposes probing IC by studying events containing a Z boson and a charm jet, Zc , in the forward region of pp collisions at the LHC. Since Zc production is inherently at large Q , and the electroweak bosons do not participate in the strong interaction, hadronic effects are small. Figure 2 shows $gc \rightarrow Zc$ scattering, a leading-order Zc production mechanism where

one of the initial partons should have large- x in the forward rapidity region. Thus, Zc production serves as a direct probe of IC in the valence quark region.

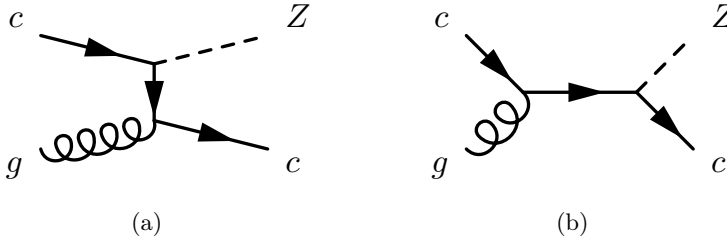


Fig. 2. Leading-order Feynman diagrams for $gc \rightarrow Zc$.

This article presents the first measurement of Zc production in the forward region using the full Run 2 data collected by LHCb in 2015, 2016, 2017, and 2018 at 13 TeV and corresponding to 6 fb^{-1} . The strategy of this analysis is to measure the ratio of production cross sections $R_j^c \equiv \sigma(Zc)/\sigma(Zj)$, where Zj refers to events containing a Z boson and any type of jet. The ratio is chosen because it is less sensitive to experimental and theoretical uncertainties than $\sigma(Zc)$. The Z bosons are reconstructed using the $Z \rightarrow \mu^+\mu^-$ decay in the mass range $60 < m(\mu^+\mu^-) < 120 \text{ GeV}$. The quantity R_j^c is measured as $R_j^c = N(c\text{-tag})/[\epsilon_{c\text{-tag}}N(j)]$, where $N(c\text{-tag})$ is the observed Zc yield, $\epsilon_{c\text{-tag}}$ is the c -tagging efficiency, and $N(j)$ is the total Zj yield.

Figure 3 shows the measured R_j^c distribution in bins of Z rapidity (y_Z). The ratio is determined to be $4.98 \pm 0.25(\text{stat.}) \pm 0.35(\text{syst.})$ in the range of $2.0 < y_Z < 4.5$. NLO SM predictions for R_j^c without IC [9], allowing

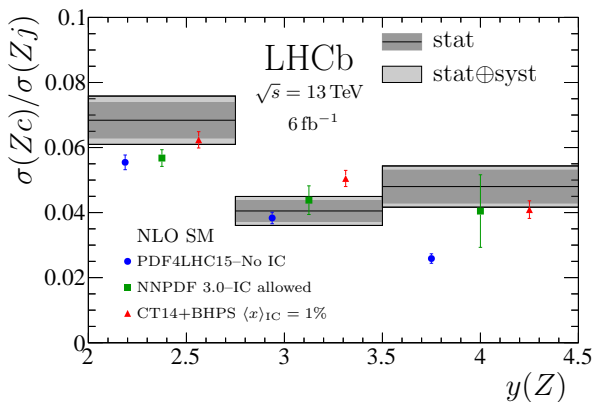


Fig. 3. Measured R_j^c distribution compared to NLO SM predictions without IC, with the c -quark PDF shape allowed to vary, and with IC as predicted by BHPS with a mean momentum fraction of 1%.

for potential IC [10], and with the valence-like IC predicted by BHPS with a mean momentum fraction of 1% [11] are also given and compared with the measurements. The observed ratios are consistent with both the no-IC and IC hypotheses in the first two y_Z bins, whereas it is not the case in the most forward bin where valence-like IC is expected to cause a large enhancement. The observed R_j^c value is significantly larger than the no-IC-expected calculation and is consistent with the calculations including the IC.

3. Probe cold nuclear matter effects: Z production in proton–lead collisions

The production of electroweak bosons at hadron colliders is an important benchmark process. Because electroweak bosons do not participate in the strong interaction, they are not affected by the QCD medium created in proton–lead collisions. Therefore, electroweak bosons preserve the initial conditions of the collisions and can be used to probe cold nuclear matter effects and constrain nPDFs [12, 13] inside nuclei.

This article presents the measurements of the $Z \rightarrow \mu^+\mu^-$ production in proton–lead collisions at the LHCb using data samples collected at a center-of-mass energy of 8.16 TeV. The dataset corresponds to an integrated luminosity of $12.2 \pm 0.3 \text{ nb}^{-1}$ for forward ($p\text{Pb}$) collisions and $18.6 \pm 0.5 \text{ nb}^{-1}$ for backward ($\text{Pb}p$) collisions. The fiducial cross section of the $Z \rightarrow \mu^+\mu^-$ production is measured using the formula $\sigma_{Z \rightarrow \mu^+\mu^-} = (N_{\text{cand}} \rho f_{\text{FSR}}) / (\mathcal{L} \epsilon_{\text{tot}})$, where N_{cand} is the number of $Z \rightarrow \mu^+\mu^-$ candidates after signal selection, ρ is the signal purity, f_{FSR} is final-state radiation correction, \mathcal{L} is the integrated luminosity, and ϵ_{tot} is the total efficiency. The fiducial region is defined as $60 < m_{\mu^+\mu^-} < 120 \text{ GeV}$, where both muons satisfy $p_T > 20 \text{ GeV}$ and $2 < \eta < 4.5$. The total fiducial cross section of the Z production in forward and backward collisions is measured to be $\sigma_{Z \rightarrow \mu^+\mu^-, p\text{Pb}} = 26.9 \pm 1.6 \text{ (stat.)} \pm 0.9 \text{ (syst.)} \pm 0.7 \text{ (lumi.) nb}$ and $\sigma_{Z \rightarrow \mu^+\mu^-, \text{Pb}p} = 13.4 \pm 1.0 \text{ (stat.)} \pm 0.5 \text{ (syst.)} \pm 0.3 \text{ (lumi.) nb}$.

The forward-to-backward production ratio, R_{FB} , is sensitive to nuclear effects in the $Z \rightarrow \mu^+\mu^-$ production. The R_{FB} ratio in the common Z -boson rapidity acceptance window is measured to be 0.78 ± 0.10 . Comparing the cross sections between proton–lead and pp collisions, the nuclear modification factors ($R_{p\text{Pb}}$) are also calculated. The measured nuclear modification factors are 0.94 ± 0.07 and 1.20 ± 0.11 for forward and backward rapidities, respectively.

Figure 4 shows the measured Z -boson cross section, R_{FB} and $R_{p\text{Pb}}$, compared to the POWHEG [14–16] calculations of the CTEQ61 proton PDF set, EPPS16 nPDF, and nCTEQ15 nPDF sets. The differential results as a function of Z rapidity in the centre-of-mass frame (y_Z^*), the transverse

momentum (p_T^Z), and an angular variable ϕ^* can be found in Ref. [4]. The variable ϕ^* [17] is defined as $\phi^* = \tan(\pi/2 - |\Delta\phi|/2) / \cosh(\Delta\eta/2)$, where the $\Delta\phi$ is a difference between the azimuthal angle of the two-muon momenta, the $\Delta\eta$ is a difference between the pseudorapidity of the two muons.

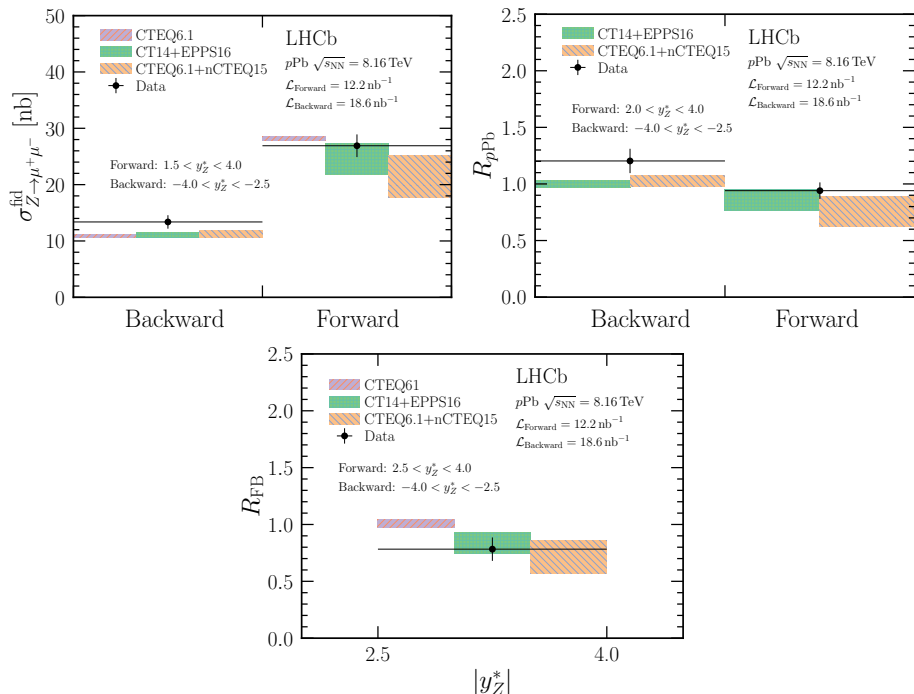


Fig. 4. The measured overall Z -production fiducial cross section (top left), the measured nuclear modification factor (top right), and the measured forward-backward ratio (bottom), compared with the PowhegBox prediction using CTEQ61, EPS16, and nCTEQ15 (n)PDF sets, for forward and backward collisions, respectively.

4. Conclusions

In these proceedings, we present the first measurement of events containing Z boson and a charm jet in the forward region of pp collisions at 13 TeV. The ratio R_j^c as a function of y_Z is measured and compared to NLO SM calculations. The observed R_j^c shows a sizable enhancement in forward y_Z , consistent with the expectation of an intrinsic charm presence.

Z -boson production in $p\text{Pb}$ collisions can probe the cold nuclear matter effects. This article presents the measurements of the Z -boson production in proton-lead collisions at 8.16 TeV at the LHCb. The Z -boson production fiducial cross section, R_{FB} and $R_{p\text{Pb}}$, are measured integrated

and differentially as a function of y_Z^* , p_T^Z , and ϕ^* . These results are compatible with theoretical predictions of the EPPS16 and nCTEQ15 nPDFs. The measurements are also compatible with previous results from the LHCb experiments at 5.02 TeV [18] but more precise. Furthermore, the forward measurements show strong constraining power for the nPDFs, especially on the high-rapidity region (small Bjorken- x).

REFERENCES

- [1] LHCb Collaboration, *J. Instrum.* **3**, S08005 (2008).
- [2] LHCb Collaboration, *Int. J. Mod. Phys. A* **30**, 1530022 (2015).
- [3] LHCb Collaboration (R. Aaij *et al.*), *Phys. Rev. Lett.* **128**, 082001 (2022).
- [4] LHCb Collaboration, [arXiv:2205.10213 \[hep-ex\]](#).
- [5] S.J. Brodsky *et al.*, *Adv. High Energy Phys.* **2015**, 231547 (2015).
- [6] S.J. Brodsky *et al.*, *Phys. Lett. B* **93**, 451 (1980).
- [7] S.J. Brodsky *et al.*, *Phys. Rev. D* **23**, 2745 (1981).
- [8] T. Boettcher, P. Ilten, M. Williams, *Phys. Rev. D* **93**, 074008 (2016).
- [9] T.-J. Hou *et al.*, *J. High Energy Phys.* **1802**, 59 (2018).
- [10] NNPDF Collaboration, *Eur. Phys. J. C* **76**, 647 (2016).
- [11] NNPDF Collaboration, *Eur. Phys. J. C* **77**, 663 (2017).
- [12] A. Kusina *et al.*, *Eur. Phys. J. C* **77**, 488 (2017).
- [13] K.J. Eskola *et al.*, *Eur. Phys. J. C* **77**, 163 (2017).
- [14] P. Nason, *J. High Energy Phys.* **2004**, 040 (2004).
- [15] S. Frixione *et al.*, *J. High Energy Phys.* **2007**, 070 (2007).
- [16] S. Alioli *et al.*, *J. High Energy Phys.* **2010**, 43 (2010).
- [17] M. Vesterinen, T.R. Wyatt, *Nucl. Instrum. Methods Phys. Res. A* **602**, 432 (2009).
- [18] LHCb Collaboration, *J. High Energy Phys.* **2014**, 30 (2014).